Broadband coherent anti-Stokes Raman scattering light generation in BBO crystal by using two crossing femtosecond laser pulses

Jun Liu,[1,2] Jun Zhang,[1] and Takayoshi Kobayashi[1,2,3,4,*]

[1]*Department of Applied Physics and Chemistry and Institute for Laser Science, University of Electro-Communications, Chofugaoka 1-5-1, Chofu, Tokyo 182-8585 Japan*
[2]*International Cooperative Research Project (ICORP), Japan Science and Technology Agency, 4-1-8 Honcho, Kawaguchi, Saitama 332-0012, Japan*
[3]*Department of Electrophysics, National Chiao Tung University, 1001 Ta Hsueh Road, Hsinchu 300, Taiwan*
[4]*Institute of Laser Engineering, Osaka University, Yamadakami 2-6, Suita 565-0871, Ibaraki 567-0047, Japan*
**Corresponding author: kobayashi@ils.uec.ac.jp*

Received April 1, 2008; accepted May 10, 2008;
posted May 29, 2008 (Doc. ID 94396); published June 26, 2008

As broad as 12000 cm^{-1} coherent anti-Stokes Raman scattering (CARS) light from ultraviolet to infrared was generated in a BBO crystal by using two crossing femtosecond laser pulses with 30% conversion efficiency. More than fifteenth-order anti-Stokes and second-order Stokes Raman sidebands were observed with nice Gaussian spatial mode. The effect of the crossing angle between two input beams on the spectrum and emitting angle of the Raman sidebands was studied in detail. Calculation shows that the phase-matching condition determines the frequencies and angles of the sidebands. © 2008 Optical Society of America

OCIS codes: 190.5650, 190.5890, 190.4720, 320.2250.

In the past decade, collinear high-order stimulated Raman scattering (RS) [1] and high-order harmonic generation (HHG) [2] have been extensively studied to generate ultrabroadband spectra for the purpose of generating subfemtosecond light pulses. Although subfemtosecond pulses have been generated by means of HHG extensively [3], RS still offers an attractive alternative to obtain ultrashort pulse owing to its higher conversion efficiency than HHG. A 1.6 fs ultrashort pulse has been generated through Fourier synthesis of several discrete Raman sidebands of cooled D_2 gas [4]. Recently, a similar RS phenomenon was found even in solid-state materials by using two crossing femtosecond laser beams, such as $YFeO_3$ [5], $SrTiO_3$ [6], $KTaO_3$ [7], $LiNbO_3$ [8], $KNbO_3$ [9], and TiO_2 [10], all at room temperature. As many as 20 anti-Stokes (AS) and 2 Stokes (S) coherent beams were generated in a lead tungstate ($PbWO_4$) very recently [11], and this kind of RS could be selectively excited by using a pair of time-delayed linearly chirped pulses [12].

Here, we report broadband high-order coherent anti-Stokes RS generation in a BBO crystal. This is very interesting, because BBO crystal is the most frequently used crystal in few-cycle ultrashort femtosecond pulse generation in visible by means of noncollinear optical parametric amplification [13–15].

A femtosecond laser system (Micra+Legend –USP) produces 2.5 mJ, 40 fs, and 1 kHz pulses centered around 800 nm. The laser pulses were divided into two beams by a beam splitter. One beam (beam 1) was spectrum broadened in a hollow fiber and then was dispersion compensated with a chirped-mirror pair and a pair of glass wedges. The other beam (beam 2) passed through a delay stage with better than 3 fs resolution. The two laser beams were attenuated by a variable neutral-density (ND) filter and then focused into a 2-mm-thick BBO (type I, $\theta=21^\circ$, $\phi=0^\circ$) crystal. The laser polarizations of both beams were parallel to the optic axis of BBO. The spectra of different order CARS signal were measured by a spectrometer (USB4000) through an optical fiber attached to an arm on a moveable stage normal to the diffracted signal beam.

The laser spectrum after the hollow fiber extended from 660 to 900 nm. The pulse before the crystal was positively chirped to about 100 fs duration owing to the variable ND filter and the glass wedge pair. At first the crystal was placed before the focal point of a lens. The beam diameters of both beams on the crystal were measured to be about 0.8 mm. The pulse energies on the BBO crystal were 40 μJ (beam 2) and 54 μJ (beam 1). The angle between the two beams in the air was 1.75° and nearly normal to the surface of the crystal. When the two laser beams were well overlapped temporally and spatially, multiple bright sidebands were generated on both sides of the two input beams. A photograph of sidebands light on a white sheet of paper placed behind the BBO crystal is shown at the top of Fig. 1(a). As many as 15 AS sidebands and 2 S sidebands were generated, and they were well separated spatially. The spectra of different order RS signal were also measured and shown in Fig. 1(c). The spectrum of the sidebands can extend from the ultraviolet to the infrared with more than 1 octave. When the delay time of beam2 was tuned less than 20 fs, multiple AS sidebands moved to the side of beam2 [Fig. 1(b)]. In this case, beam2 was used as a pump. The wavelengths of the same order sidebands were shifted when the AS sidebands emit on the different side of the two input beams. The frequency spacings between two neighboring sidebands were also different between the signals shown in Figs. 1(a) and 1(b).

Dependence of the sideband spectra on the crossing angle was studied by changing the direction of the

0146-9592/08/131494-3/$15.00

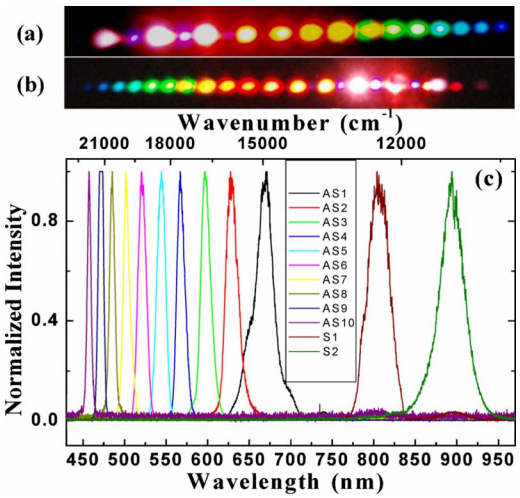

Fig. 1. (Color online) Photograph of the sidebands in a white sheet of paper behind the BBO crystal when (a) beam1 works as a pump and (b) beam2 works as a pump. (c) Spectra of sidebands from Fig. 1(a); A Sm (m=1–10) refers to the mth-order anti-Stokes spectrum, and Sn (n=1,2) refers to the mth-order Stokes spectrum.

beam1 with a fixed direction of beam2. In the experiment, two beams were set at five different crossing angles in the air: 1.53°, 1.75°, 2.18°, 2.62°, and 3.05°. The spectra of the sidebands and the conversion efficiency were found to be changed by varying the crossing angle. This phenomenon was also reported recently by Zhi and Sokolov [11]. The brightest sideband signals were observed when the crossing angle was set at 1.75°. As the crossing angle was decreased, the sidebands became close to each other both in frequency and space. A weak continuous line was generated when the crossing angle was reduced to smaller than 1.0°. The frequency spacing between the two neighboring sidebands increased gradually with the crossing angle. The spectrum of AS1 at different crossing angles is shown in the inset of Fig. 2. The spectrum of AS1 was shifted to high frequency when the crossing angle was increased. We could see that the center wavelength of the sidebands can be tuned in a large bandwidth simply by changing the crossing angle. As the sideband order increased, the frequency separation between the two neighboring sidebands gradually decreased, as shown in Fig. 2. The frequency spacing between AS1 and AS2 was about 1117 cm^{-1} for 2.18° crossing angle, which is gradually decreasing to 691 cm^{-1} for AS8 and AS9.

In the CARS process, the laser beams should obey the energy conservation and momentum conservation laws: $\omega_{AS}=2\omega_p-\omega_s$ and $2\vec{k}_p-\vec{k}_s-\vec{k}_{AS}=0$, respectively, as shown in Fig. 3. Here, s and p (seed and pump) refer to the two input laser beams, while AS refers to the generated sidebands. Using the two conservation laws, the dependence of the AS1 wavelength on the crossing angle were calculated, the results being shown in Fig. 3. In the calculation, we fix the wavelength of s at 800 nm and vary the wavelength of p light from 660 to 780 nm to accord with the two input beams under the experiment condition. It can be seen that the calculated results agree very well with the experiment results. Therefore, frequency dependence on the angle can be explained in terms of the phase matching. High conversion efficiency is obtained when the crossing angle is around 2°. It is because the frequency difference between the p and s in the calculation is close to the broad Raman line at 1547 cm^{-1} [16], and it is enhanced by the difference-frequency resonance as in the ordinary Raman process. The observed frequencies of Raman shift are different from the Raman shift measured by the conventional Raman spectrum [16]. This is probably because the four-wave mixing process is taking place being associated with optical phonon mode, which satisfies the phase-matching condition [9,10].

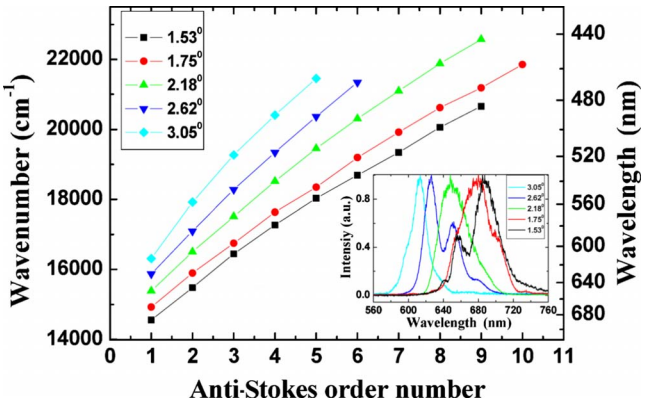

Fig. 2. (Color online) Center wavenumber (wavelength) of different sidebands varies with the anti-Stokes order number when the crossing angle between two input beams is 1.53°, 1.75°, 2.18°, 2.62°, and 3.05°. The inset shows the spectra of the first-order sidebands when the crossing angles between the two beams are 1.53°, 1.75°, 2.18°, 2.62°, and 3.05°.

The dependence of the center wavenumber and wavelength of different order AS on the emitting angle at different crossing angles is plotted in Fig. 4. As can be seen, the slope for center wavenumber to output angle is almost constant, which is about

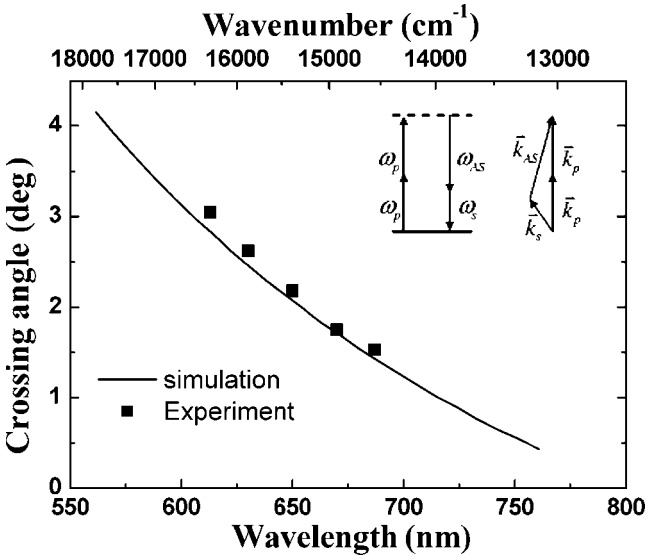

Fig. 3. Dependence of peak wavelength of the first-order AS sidebands on the crossing angle of two input beams. The crossing angle was measured in the air. Squares, experimental results. Curve, calculated results by using the phase-matching condition.

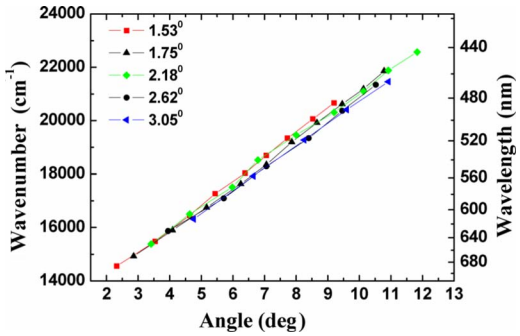

Fig. 4. (Color online) Relationship between the center wavenumber (wavelength) of different sidebands and the emitting angle of different sidebands. The crossing angles between the two input beams of which direction is normal to the crystal surface are 1.53°, 1.75°, 2.18°, 2.62°, and 3.05°.

843 cm^{-1}/deg. This means that the emitting angle of sidebands is not related to the AS number but to the center wavelength of the sidebands. This linear relationship between the emitting angle and the wavelength of sidebands makes it possible to synthesize these sidebands by using dispersion optics that has been recently realized by Matsubara *et al.* [8].

When the crystal was located on the focal point of the lens, the beam diameter was measured to be about 200 μm. When the energy of each incident laser pulse was 3μJ, bright sidebands were also observed. The spatial profile of the sidebands was also measured by using a CCD camera behind the crystal. Figure 5 shows a spatial profile of the AS2 and AS3 sideband signals. The figure also shows the spectrum of pump laser with and without the seed. The conversion efficiency of pump into the sidebands was higher than 30%, as also can be seen from spectral intensity of pump pulse with and without the seed in Fig. 5. There was almost no dependence of the spectrum of the first-order AS sidebands on the phase-match angle (θ) within ±15°. There was no sidebands generation when the polarization of one input beam was rotated 90°.

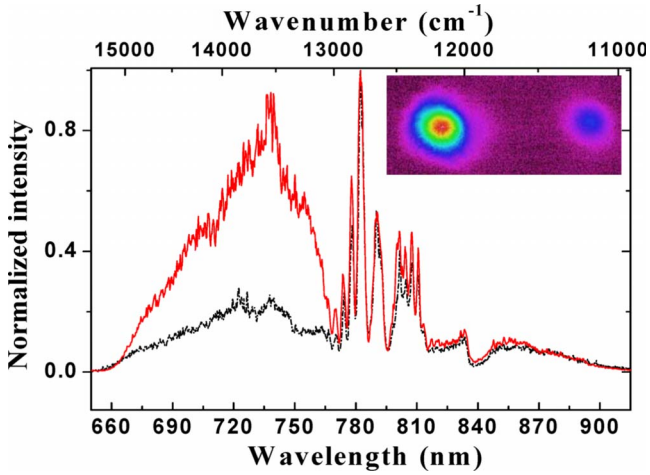

Fig. 5. (Color online) Spectrum of the pulse after the hollow fiber compressor (solid curve) and the spectrum of the pulse after the BBO crystal with CARS effect (dotted curve). The inset is the photograph showing the spatial profile of the second-order (left) and the third-order (right) sidebands.

In summary, we have observed a broadband CARS signal generation in a most frequently used nonlinear crystal BBO pumped by using two crossing femtosecond laser pulses. More than 1 octave spectrum from ultraviolet to infrared was obtained in this way. The energy conversion efficiency in this kind of nonlinear process is about 30% in the experiment. The phase matching in crystal plays an important role in the CARS process. This phenomenon will extend the possible application of BBO crystal in a new device. Subfemtosecond light may be able to be obtained by synthesizing this kind of sideband in the future.

The authors thank Miaochan Zhi for his helpful discussion and Zhiguang Wang for his technical assistance.They also thank Eiichi Hanamura for his valuable discussion. This work was partly supported by the grant from the Ministry of Education in Taiwan under the ATU Program at National Chiao Tung University. A part of this work was performed under the joint research project of the Laser Engineering, Osaka University, under contract subject B1-27.

References

1. A. V. Sokolov, M. Y. Shverdin, D. R. Walker, D. D. Yavuz, A. M. Burzo, G. Y. Yin, and S. E. Harris, J. Mod. Opt. **52**, 285 (2005).
2. M. Hentschel, R. Kienberger, Ch. Spielmann, G. A. Reider, N. Milosevic, T. Brabec, P. Corkum, U. Heinzmann, M. Drescher, and F. Krausz, Nature **414**, 509 (2001).
3. R. Kienberger, E. Goulielmakis, M. Uiberacker, A. Baltuska, V. Yakovlev, F. Bammer, A. Scrinzi, Th. Westerwalbesloh, U. Kleineberg, U. Heinzmann, M. Drescher, and F. Krausz, Nature **427**, 817 (2004).
4. M. Y. Shverdin, D. R. Walker, D. D. Yavuz, G. Y. Yin, and S. E. Harris, Phys. Rev. Lett. **94**, 033904 (2005).
5. J. Takahashi, E. Matsubara, T. Arima, and E. Hanamura, Phys. Rev. B **68**, 155102 (2003).
6. J. Takahashi, M. Keisuke, and Y. Toshirou, Opt. Lett. **31**, 1501 (2006).
7. E. Matsubara, K. Inoue, and E. Hanamura, Phys. Rev. B **72**, 134101 (2005).
8. E. Matsubara, T. Sekikawa, and M. Yamashita, Appl. Phys. Lett. **92**, 2008, 071104 (2008).
9. H. Matsuki, K. Inoue, and E. Hanamura, Phys. Rev. B **75**, 024102 (2007).
10. K. Inoue, J. Kato, E. Hanamura, H. Matsuki, and E. Matsubara, Phys. Rev. B **76**, 041101(R) (2007).
11. M. Zhi and A. V. Sokolov, Opt. Lett. **32**, 2251 (2007).
12. M. Zhi and A. V. Sokolov, New J. Phys. **10**, 025032 (2008).
13. A. Baltuska, T. Fuji, and T. Kobayashi, Opt. Lett. **27**, 306 (2002).
14. A. Shirakawa, I. Sakane, M. Takasaka, and T. Kobayashi, Appl. Phys. Lett. **74**, 2268 (1999).
15. A. Shirakawa, I. Sakane, and T. Kobayashi, Opt. Lett. **23**, 1292 (1998).
16. J. L. You, G. C. Jiang, H. Y. Hou, Y. Q. Wu, H. Chen, and K. D. Xu, Chin. Phys. Lett. **19**, 205 (2002).